Acta Orthop. Scand. *58*, 499–503, 1987

Magnetic resonance imaging and histopathology in femoral head necrosis

Yoshio Takatori, Morihide Kamogawa, Takashi Kokubo[1], Toshitaka Nakamura, Setsuo Ninomiya, Kouki Yoshikawa[1] & Hajime Kawahara

We correlated preoperative magnetic resonance (MR) images and histopathology of eight femoral heads from patients with osteonecrosis. The signal intensity of the MR image was low in the area where fibrovascular tissue, disintegrated fibrovascular tissue, or amorphous necrotic material occupied the medullary space. On the other hand, the necrotic marrow without revascularization showed high signal intensity. Osteonecrosis can be detected by MR imaging as soon as a certain amount of bone marrow is replaced by fibrovascular tissue.

Recent reports have documented the possibility of magnetic resonance (MR) imaging for specifying the affected area of osteonecrosis in the femoral head (Moon et al. 1983, Totty et al. 1984). Totty et al. (1984) suggested that death of the fat cells caused a decrease in signal intensity. We correlated the preoperative MR images with the histopathologic findings in femoral head necrosis.

Patients and methods

Eight femoral heads from 6 patients with osteonecrosis were replaced with prostheses within 6 weeks after MR imaging at the University of Tokyo Hospital from May 1985 to March 1986 (Table 1). Cases 1 and 6 were replaced bilaterally. On plain radiography, all but Case 6 were Stage

Table 1. Clinical data for 6 patients with necrosis of the femoral head

Specimen	Case	Sex	Age	Side	Time between onset of symptoms and investigation (yr)	Etiology
1	1	M	27	L	3	Systemic lupus erythematosus
2				R	2.5	
3	2	M	77	L	0.5	Idiopathic osteonecrosis
4	3	M	27	L	2	Nephrotic syndrome
5	4	F	75	R	1	Idiopathic osteonecrosis
6	5	M	44	L	3.5	Central retinitis
7	6	M	45	L	0.5	Alcoholism
8				R	0.5	

Departments of Orthopedics and [1]Radiology, Faculty of Medicine, University of Tokyo, Japan

Correspondence: Dr. Yoshio Takatori, Hakusan-Ekuseruhaimu 703, 2-26-16 Hakusan, Bunkyo-ku, Tokyo-112, Japan

Figure 1

A

B

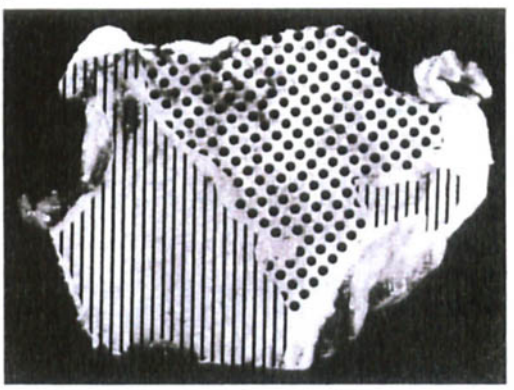

C

Figure 1. Specimen 2. Case 1.
A. Preoperative MR image. Low signal-intensity area occupied proximal two thirds of femoral head.
B. Succino-dehydrogenase test. Unstained area was smaller than low signal-intensity area on MR image.
C. Dotted area represented fibrovascular tissue, disintegrated fibrovascular tissue, or amorphous necrotic material. Vertically lined area represented bone marrow tissue. Dotted area corresponded to low signal-intensity area on MR image.

Figure 2

A

B

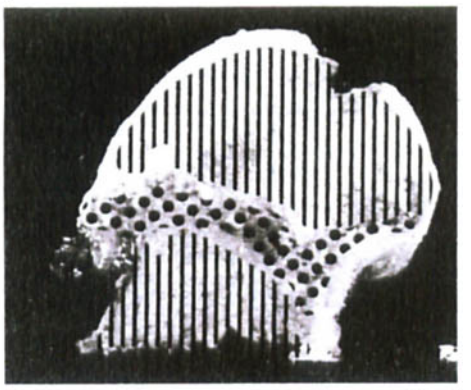

C

D

Figure 2. Specimen 8. Case 6.
A. Preoperative MR image. Low signal-intensity area showed bandlike pattern.
B. Succino-dehydrogenase test. Proximal half was not stained. Unstained area was obviously different from low signal-intensity area on MR image.
C. Dotted area represented fibrovascular tissue, disintegrated fibrovascular tissue, and amorphous necrotic material. Vertically lined area represented bone marrow tissue. Dotted area corresponded to low signal-intensity area on MR image.
D. Oil red O method. Unstained area corresponded to low signal-intensity area on MR image.

4 according to the classification of Arlet et al (1971). In Case 6, both heads had collapsed with intracapital fracture and displacement on the left side (Figure 1). 99mTechnetium bone scanning was performed in Cases 1, 4, and 5, with increased uptake in all of them.

MR images with an image plane of 10-mm thickness were displayed with 256 × 256 matrix elements by a Siemens Magnetom superconductive magnet operating in a spin-echo technique with a repetition time of 600 and 1,600 msec and an echo time of 35 and 70 msec at 1.5 tesla. Thus, four different pulse sequences were employed. The coronal images centered at the femoral head and neck were used for the study. We obtained the T1 calculated image from spin echos 600/35 and 1600/35 sequences and the T2 calculated image from spin echos 600/35 and 600/70 sequences in Cases 1, 3, 4, and 5. Setting the region of interest (ROI) in the display, we measured T1 and T2 values of low signal-intensity areas and compared them with those of 10 femoral heads from 5 normal volunteers. For analyses the Wilcoxon signed-rank test was used.

An 8-mm-thick slab was taken from each femoral head corresponding to the preoperative coronal MR images. In specimens 7 and 8, a neighboring 2-mm-thick slab was taken for lipid staining. The 8-mm-thick slab was examined radiographically by Softex CBM (Softex Co.) and biochemically by the succino-dehydrogenase test (Merle D'Aubigné et al. 1965). Then, the slab was fixed in a 10 per cent neutral buffered formalin solution for 2 weeks and demineralized in a Plank-Rychlo solution for 2–5 days. Next, the slab was neutralized and washed in floating water. After paraffin embedding, two 5-μ-thick sections were taken from each surface of the slab. In specimens 3, 4, and 7, the slabs were divided in the coronal plane into two slices after demineralization, and two sections each were taken from the four surfaces of the specimen. Then, these four or eight sections from each slab were stained with hematoxylin and eosin. At microscopy, four different structures were identified in the medullary space: bone marrow, fibrovascular tissue, disintegrated fibrovascular tissue, and amorphous necrotic material. Fat cells with normal architecture suggested preservation of bone marrow. The disintegrated fibrovascular tissue was characterized by cells that lost their clear margin and stainability of the nucleus. According to the histologic constitution of these sections, that of the slab was reconstructed. If different tissues occupied the corresponding area of these sections, the area was omitted from reconstruction. Then, we compared topologically the histological constitution of the slab with the MR image.

To study the distribution of fat in the femoral head, another 2-mm-thick slab of specimens 7 and 8 was used. The slab was imprinted with a roller on a piece of Japanese paper, which was flexible and tough in water. Thus, three pieces of paper were obtained from each specimen and stained for lipid by oil red O, Nile blue, and pancreatic lipase methods (Adams et al. 1965).

Results

All four pulse sequences revealed an area of low signal intensity in the affected femoral head. Using the spin echo 600/35 sequence, we could define this area most clearly, in which also the T1 relaxation time was prolonged (Table 2).

By the succino-dehydrogenase test, the proximal part of the slab was not stained in all the specimens. In specimens 1–6, the unstained area was smaller than the area of low signal intensity, which occupied the proximal part of the femoral head (Figure 1). In specimens 7 and 8, the unstained area was obviously different from the area of low signal intensity, which showed a band-like pattern (Figure 2).

In specimens 1 and 3, an area of low signal intensity occupied the femoral head except for the most distal part. Microscopically, the proximal half of the specimen was occupied by disintegrated fibrovascular tissue and amorphous necrotic material, and the distal half by fibrovascular tissue. Bone marrow was found only in the most distal part of the specimen. In specimens 2, 4, 5, and 6, low signal intensity was found in the

Table 2. Comparison of T1 and T2 values (msec) of normal femoral head and low signal-intensity area of osteonecrosis. Mean (SD)

	T1	T2
Normal femoral head (n 10)	363(53)	39.8(5.3)
	P<0.01	NS
Osteonecrosis (n 5)	1491(838)	54.3(19.4)

proximal part and high intensity in the distal part (Figure 1). Microscopically, bone marrow occupied the distal part of the specimen. Fibrovascular tissue spread proximally from the bone marrow and adjoined disintegrated fibrovascular tissue and amorphous necrotic material (Figure 1). In these specimens the boundary between the two different intensity areas on the MR images corresponded to that between bone marrow and fibrovascular tissue. In specimens 7 and 8, a band of low signal intensity was found (Figure 2). Microscopically, this band consisted of fibrovascular tissue, disintegrated fibrovascular tissue, and amorphous necrotic material, which was interposed between the proximal and distal areas of the bone marrow (Figure 2). The cells of the bone marrow in the proximal part had lost nuclear staining, suggesting cell death. As a result, the signal intensity of the MR image was high for bone marrow and low for fibrovascular tissue, disintegrated fibrovascular tissue or amorphous necrotic material.

By the three lipid staining methods, a band was not stained in specimens 7 and 8. This unstained area corresponds well to the area of low signal intensity (Figure 2).

Discussion

The MR-anatomic correlation has been studied on the vertebral disc (Peck & Haughton 1985), the uterus (Lee et al. 1985), and the knee joint (Reicher et al. 1985). However, the MR imaging was performed on the removed specimens; and in vivo and in vitro MR images are not always the same. Therefore, we compared the in vivo MR images with the histopathologic findings of the specimens.

The succino-dehydrogenase test reflects the activities of the mitochondrial enzymes (Nachlas et al. 1957). However, the unstained area was obviously smaller than the area of low signal intensity in specimens 1–6. Moreover, the proximal parts of specimens 7 and 8 had high signal intensity. These results show that the MR images do not directly represent "the necrosis."

It has been described that the physeal scar and the prominent central weight-bearing trabeculae are represented as a low signal-intensity line and band (Totty et al. 1984). Therefore, we considered that loss of high signal intensity should be attributed to a change of the medullary space. That was why we choose the medullary space for comparison with the MR image. Because of the difference in thickness of the MR and microscopy, only specimens where one kind of tissue existed throughout the thickness of the MR image were chosen for comparison.

The difference in signal intensity between bone marrow and the other tissues was compatible with the results of the succino-dehydrogenase test. It is noteworthy that the necrotic marrow without revascularization showed high signal intensity.

In specimens 7 and 8 the low signal-intensity band on the MR image corresponded well to the unstained area for lipid. According to Mizuta & Yamasaki (1984), the lipid signal was observable in ^{1}N-NMR spectra of normal tibial bone marrow from a rabbit. Therefore, the results suggest that loss of triglyceride esters causes the decrease in signal intensity. In specimens 7 and 8, we suppose that the cells of the proximal part of the femoral head had died previously, but the fat in the bone marrow remained and maintained high signal intensity. Thus, it is not death of the fat cells, but the repair process that replaces the fat that decreases signal intensity. We suppose that T1 relaxation time of fibrovascular tissue is long enough to decrease the signal intensity of the femoral head.

From this study, we believe that osteonecrosis can be detected by MR imaging as soon as the fibrovascular tissue has invaded the medullary space and replaces a certain amount of bone marrow.

References

Adams C W M, Abdulla Y H, Bayliss O B, Weller R O. Histochemical detection of triglyceride esters with specific lipases and a calcium lead sulphide technique. J Histochem Cytochem 1966;14(5):385–95.

Arlet J, Ficat P, Durroux R. Formes anatomo-cliniques (radiologiques et etiologiques) de l'ischemie chronique et de l'osteonecrose, dites primitives, de l'epiphyse femorale superieure. Rev Rhum Mal Osteoartic 1971;38(1):41–9.

Lee J K T, Gersell D J, Balfe D M, Worthington J L, Picus D, Gapp G. The uterus: in vitro MR anatomic correlation of normal and abnormal specimens. Radiology 1985;157(1):175–9.

Merle D'Aubigné R, Postel M, Mazabraud A, Massias P, Gueguen J. Idiopathic necrosis of the femoral head in adults. J Bone Joint Surg (Br) 1965;47(4):612–33.

Mizuta H, Yamasaki M. Nuclear magnetic resonance studies on experimental malignant bone tumors. Nippon Seikeigeka Gakkai Zasshi 1984;58(1):83–95.

Moon K L Jr, Genant H K, Davis P L, Chafetz N I, Helms C A, Morris J M, Rodrigo J J, Jergesen H E, Brasch R C, Bovill E G Jr. Nuclear magnetic resonance imaging in orthopaedics: principles and applications. J Orthop Res 1983;1(1):101–14.

Nachlas M M, Tsou K C, de Souza E, Cheng C S, Seligman A M. Cytochemical demonstration of succinic dehydrogenase by the use of a new p-nitrophenyl substituted ditetrazole. J Histochem Cytochem 1957;5:420–36.

Pech P, Haughton V M. Lumbar intervertebral disk: correlative MR and anatomic study. Radiology 1985;156(3):699–701.

Reicher M A, Rauschning W, Gold R H, Bassett L W, Lufkin R B, Glen W Jr. High resolution magnetic resonance imaging of the knee joint: normal anatomy. AJR 1985;145(5):895–902.

Totty W G, Murphy W A, Ganz W I, Kumar B, Daum W J, Siegel B A. Magnetic resonance imaging of the normal and ischemic femoral head. AJR 1984;143(6):1273–80.

Acknowledgements

The authors would like to thank Professor T. Kurokawa for his kind advice. The authors are indebted to Drs. Y. Kariya, K. Nishimura, Y. Miyanaga, and Y. Nagata for their assistance.